ELSEVIER

The methylene saga continues: Stretching fundamentals and zero-point energy of $\tilde{X}^3B_1$ CH$_2$ ☆

Tibor Furtenbacher[a], Gábor Czakó[a], Brian T. Sutcliffe[a], Attila G. Császár[a,☆], Viktor Szalay[b]

[a]Department of Theoretical Chemistry, Eötvös University, P.O. Box 32, H-1518 Budapest 112, Hungary
[b]Crystal Physics Laboratory, Research Institute for Solid State Physics and Optics, Hungarian Academy of Sciences, P.O. Box 49, H-1525 Budapest, Hungary

Abstract

The vibrational fundamentals and the rotational levels up to $J = 7$ of the $\tilde{X}^3B_1$ and $\tilde{a}^1A_1$ electronic states of CH$_2$ have been computed completely ab initio. The calculations were based on converged, variational nuclear motion calculations employing high-quality ab initio quartic force field approximations of the related potential energy surfaces (PES). The vibrational fundamentals obtained are compared to other computational results, namely those obtained from second-order vibrational perturbation theory (VPT2) and the nonrigid-rotation-large-amplitude-internal-motion Hamiltonian (NRLH) approach. The variationally computed rotational transitions are compared both to experimentally available results and to results obtained using empirical, fitted PESs. The comparisons suggest that while the fitted PESs of $\tilde{X}^3B_1$ CH$_2$ reproduce excellently the available rovibrational transition wavenumbers, the corresponding stretching fundamental term values, which have not been determined experimentally, are less accurate than the ab initio values obtained in the present study. This means that the zero-point energy (ZPE) computed ab initio in the present work is an improvement over that computed from the fitted PES of $\tilde{X}^3B_1$ CH$_2$. No similar problems are observed for the semirigid $\tilde{a}^1A_1$ state of CH$_2$, where the computed, the fitted, and the experimental results all agree with each other. The symmetric and antisymmetric stretching fundamentals of $\tilde{X}^3B_1$ CH$_2$ obtained in this study are 3035 ± 7 and 3249 ± 7 cm^{-1}, respectively. The corresponding ZPE of $\tilde{X}^3B_1$ is 3733 ± 10 cm^{-1}, while that of $\tilde{a}^1A_1$ CH$_2$ is 3605 ± 15 cm^{-1}.
© 2005 Elsevier B.V. All rights reserved.

1. Introduction

The unique role the simple triatomic molecule methylene (CH$_2$) has played in the development of modern quantum chemical techniques was reviewed excellently by Schaefer [1] almost two decades ago. To understand how the structure and energetics of methylene has become a 'paradigm for quantitative quantum chemistry' [1] it is sufficient to mention that two important results, deduced by some of the best spectroscopists in the world [2–5] namely that triplet methylene has a linear equilibrium structure [2]

and that the singlet-triplet energy separation, T_o ($\tilde{a}^1A_1$), is either small, around 2 kcal mol^{-1} [3,4], or large, almost 20 kcal mol^{-1} [5], proved to be even qualitatively wrong by theory (see, e.g. Refs. [6–9] for recent compilations of relevant experimental and computational data). In both cases, it was pure ab initio electronic structure theory that provided correct answers for the relevant quantities from almost the very beginning.

From the results presented in this study it seems that the methylene saga is continued in that pure ab initio theory can now improve some of the empirical data deduced from experiment for $\tilde{X}^3B_1$ CH$_2$. As shown below, ab initio theory predicts the stretching fundamentals of the lowest triplet state of CH$_2$, so far not measured directly, and thus the subsequent zero-point energy (ZPE) of $\tilde{X}^3B_1$ CH$_2$ more accurately than some of the empirical attempts [10–17].

Recently, two of the authors of this article have been involved [6] in the definitive ab initio determination of the enthalpies of formation, both at 0 and 298.15 K, of

the two lowest electronic states of methylene, $\tilde{X}^3B_1$ and $\tilde{a}^1A_1$ [9]. Publication of Ref. [6] was severely hindered by the problem surrounding the ZPEs of the two states for which several determinations have been available in the literature. The basic problem can be described as follows. The 0–0 transition between the two states is $T_0(\tilde{a}^1A_1) = 3147 \pm 5$ cm^{-1} [11,14,16]. (A discussion of how this $T_0(\tilde{a}^1A_1)$ was determined is given in Section 6.) An accurate computational value of $T_e(\tilde{a}^1A_1) = 3262^{+29}_{-16}$ cm^{-1} was obtained in Ref. [6] after establishing the all-electron complete basis set (CBS) full configuration interaction (FCI) limit [18,19] and augmenting the result with relativistic and diagonal Born–Oppenheimer corrections (DBOC) in the spirit of the focal-point approach (FPA) [20, 21]. These T_0 and T_e values are only compatible if not the available empirical estimates [10–16], detailed below, are used for the difference between the singlet and triplet ZPEs. Rather a computational estimate [6] based on the nonrigid-rotation-large-amplitude-internal-motion Hamiltonian (NRLH) approach of Szalay [22–25] and accurate quartic force field representations of the potential energy surfaces (PES) of $\tilde{X}^3B_1$ and $\tilde{a}^1A_1$ CH$_2$ should be employed. The simplified one-dimensional treatment of Ref. [6] is substituted in this study by a fully six-dimensional variational treatment of the vibrations and rotations of both states of CH$_2$. New estimates of the vibrational fundamentals and ZPEs of ^{3}CH$_2$ and ^{1}CH$_2$ are obtained, where ^{3}CH$_2$ and ^{1}CH$_2$ are shorthand notations for $\tilde{X}^3B_1$ and $\tilde{a}^1A_1$ CH$_2$, respectively. Rotational transitions are computed with the help of an exceedingly simple algorithm and a newly developed code. These calculations help to establish the accuracy of the fitted empirical PESs of Jensen and Bunker [14], which provided significantly different estimates for the stretching fundamentals and the ZPE of ^{3}CH$_2$ but not of ^{1}CH$_2$. Here and in the following review of the literature we employ the notation ^{1}ZPE and ^{3}ZPE for the ZPEs of $\tilde{a}^1A_1$ and $\tilde{X}^3B_1$ CH$_2$, respectively, while ΔZPE refers to the ZPE difference between the excited singlet and ground-state triplet states (^{1}ZPE–^{3}ZPE).

In 1983, McKellar and co-workers [11], using the crude approximation that the stretching ZPEs are similar for the two states, determined the ZPE contribution of the bending modes of the triplet and singlet states as 670 and 499 cm^{-1}, respectively, leading to a ΔZPE of 171 cm^{-1}. Two years later, Leopold and co-workers [12], based on a ^{3}ZPE of 3430 ± 140 cm^{-1} and a ^{1}ZPE of 3530 cm^{-1}, obtained a curious ΔZPE estimate of $+100 \pm 140$ cm^{-1} from the deuterium shifts of photoelectron spectra of CH$_2^-$ and CD$_2^-$. In a subsequent study McLean and co-workers [13], using high-quality ab initio (six-electron corrected second-order configuration interaction, SOCI+Q) energy points and a variational nonrigid bender Hamiltonian approach [26], obtained 3710 ± 20 cm^{-1} for ^{3}ZPE. A value for ^{1}ZPE of 3620 ± 20 cm^{-1} was also determined by them from a fit to the available experimental data [27–29], corresponding to a

ΔZPE of -90 cm^{-1}. In 1989, Comeau and co-workers [15], based on [5s4p3d2f1g/3s2p1d] MR-CISD+Q, i.e. corrected multireference configuration interaction with all singles and doubles, PESs and the Morse oscillator rigid bender internal dynamics (MORBID) Hamiltonian approach [30], determined a ΔZPE of -125 cm^{-1}, with ^{3}ZPE and ^{1}ZPE values of 3711 and 3586 cm^{-1}, respectively. Based on small adjustments to the ab initio potential of Comeau and co-workers [15] in order to better reproduce the available rovibrational levels, Jensen and Bunker [14], again using their MORBID approach for solution of the nuclear motion problem, obtained 3689 cm^{-1} for ^{3}ZPE and 3613 cm^{-1} for ^{1}ZPE, resulting in a ΔZPE of only -76 cm^{-1}. For a long-time, these values remained the best empirical estimates for these quantities. In a recent publication, Gu and co-workers [16] investigated the effect of the Renner–Teller interaction of the $\tilde{a}^1A_1$ state with the $\tilde{b}^1B_1$ state and found that the adiabatic zero-point energy of $\tilde{a}^1A_1$ CH$_2$ changes appreciably, to 3621 cm^{-1}, by inclusion of a rotational contribution, closing ΔZPE to -68 cm^{-1}.

In our recent computational study [6], the best theoretical ZPE estimates were 3736^{+15}_{-15} and 3612^{+10}_{-10} for ^{3}ZPE and ^{1}ZPE, with a subsequent ΔZPE of -124^{+18}_{-18} cm^{-1}. Relevant computational results of some other high-quality studies are summarized in Table 1.

Many of the empirical and computational determinations of the ZPEs mentioned involved estimates of the vibrational fundamentals of the two states of CH$_2$ investigated. Of the six vibrational fundamentals only the two stretching fundamentals of ^{3}CH$_2$ have not been measured. The available harmonic [6,7,31,32], and anharmonic [6,14,17, 29,32–34] vibrational fundamentals of $\tilde{X}^3B_1$ and $\tilde{a}^1A_1$ CH$_2$ are summarized in Table 2. Note that the accuracy of the computed harmonic and anharmonic vibrational fundamentals should be judged differently for the two states. The $\tilde{a}^1A_1$ state is semirigid while the ground $\tilde{X}^3B_1$ state is much more floppy as can be inferred from the bending fundamentals of the two states, 963 and 1353 cm^{-1} for $\tilde{X}^3B_1$ and $\tilde{a}^1A_1$ CH$_2$, respectively.

As is clear from Table 2, there is little reason to deal with the vibrational fundamentals of $\tilde{a}^1A_1$ CH$_2$ in detail, as they have been measured experimentally and, furthermore, all dependable theoretical computations support the measured values (see also Ref. [6]). In order to obtain a good estimate of ΔZPE, one can concentrate on the stretching fundamentals of $\tilde{X}^3B_1$ CH$_2$, which have not been measured experimentally and determine ^{3}ZPE from a reliable variational nuclear motion calculation.

Details of the representations of the PESs of $\tilde{X}^3B_1$ and $\tilde{a}^1A_1$ CH$_2$ employed in this study are given in Section 2. The perturbational and variational approaches employed for the determination of rovibrational eigenstates are discussed in Section 3, the former, of course, rather briefly. Computed rotational transitions that can be compared to experimental data are discussed in detail

Table 1
Computational determinations of the zero-point energies, in cm^{-1}, for $\tilde{X}^3B_1$ and $\tilde{a}^1A_1$ $^{12}CH_2$[a]

Method	^{3}ZPE	^{1}ZPE	ΔZPE	References and notes
Harmonic	3822	3678	−144	All-electron cc-pVQZ UCCSD(T), Ref. [32]
Harmonic	3817	3642	−175	TZ2P CCSD(T), one frozen core and one frozen virtual, Ref. [7]
Harmonic	3808			All-electron aug-cc-pCVQZ ROCCSD(T), this work
Harmonic	3810	3637	−173	TZ2P FCI, one frozen core and one frozen virtual, Ref. [7]
VPT2[b]	3768	3625	−143	All-electron cc-pVQZ UCCSD(T), Ref. [32] and this work
VPT2[b]				All-electron aug-cc-pCVQZ ROCCSD(T), this work
NRLH	3736	3612	−124	Ref. [6], see also Ref. [25]
VAR	3734.66	3609.96	−124.7	Present work

[a] ^{3}ZPE = zero-point energy of $\tilde{X}^3B_1$ CH$_2$. ^{1}ZPE = zero-point energy of $\tilde{a}^1A_1$ CH$_2$. ΔZPE = ^{1}ZPE − ^{3}ZPE.

[b] The second-order vibrational perturbation theory (VPT2) results reported here do not include the small contributions from the constant (G_0) term of the VPT2 vibrational energy expansion [51].

in Section 4 in order to prove the adequacy of the quartic force field representations of the PESs for the purposes of this paper. Dependable values for the stretching fundamentals and zero-point energy of $^3CH_2$ are proposed in Section 5, the similar quantities for $^1CH_2$ are also reviewed here. This is followed by a discussion of $T_0(\tilde{a}^1A_1)$ in Section 6 to show that the computationally determined ΔZPE is supported by the available experimental data. In Section 7, we offer concluding remarks.

2. Representation of the PESs of CH$_2$

Three different representations of the potential energy surfaces (PES) of the ground triplet ($^3CH_2$) and the first excited singlet ($^1CH_2$) states of CH$_2$ have been employed in this study.

The internal coordinate quartic force fields of $^3CH_2$ and $^1CH_2$, computed at the all-electron cc-pVQZ [35–37] CCSD(T) [38] level, have been used in second-order

Table 2
Harmonic and anharmonic vibrational fundamentals, in cm^{-1}, of $\tilde{X}^3B_1$ and $\tilde{a}^1A_1$ CH$_2$[a]

$\tilde{X}^3B_1$ CH$_2$				References and notes
Harmonic	$\omega_1(a_1)$	$\omega_2(a_1)$	$\omega_3(b_2)$	
TZ2P CCSD(T)	3140	1131	3362	Ref. [7]
TZ2P FCI	3134	1127	3358	Ref. [7]
cc-p^{VTZ} CCSD(T)	3167	1085	3369	Ref. [31]
cc-pVQZ UCCSD(T)	3159	1099	3385	Ref. [32]
aug-cc-pCVQZ ROCCSD(T)	3148	1091	3377	Ref. [6]
Anharmonic	$\nu_1(a_1)$	$\nu_2(a_1)$	$\nu_3(b_2)$	
Expt.		963.1		Ref. [33]
Fitted empirical	2994.2	973.4	3212.0	Ref. [17], surface A
Fitted empirical	3013.2	969.6	3236.9	Ref. [17], surface C
Jensen and Bunker	2992.0	963.1	3213.5	Ref. [14]
cc-pVQZ UCCSD(T) + VPT2	3045	1019	3260	Ref. [32]
aug-cc-pCVQZ ROCCSD(T) + VPT2	3032	1011	3247	Ref. [6]
aug-cc-pCVQZ ROCCSD(T) + NRLH	3036	965	3249	Ref. [6]
aug-cc-pCVQZ ROCCSD(T) + VAR	3036	967	3252	Present work
$\tilde{a}^1A_1$ CH$_2$				
Harmonic	$\omega_1(a_1)$	$\omega_2(a_1)$	$\omega_3(b_2)$	
TZ2P CCSD(T)	2899	1414	2971	Ref. [7]
TZ2P FCI	2899	1404	2971	Ref. [7]
cc-pVQZ UCCSD(T)	2938	1407	3012	Ref. [32]
Anharmonic	$\nu_1(a_1)$	$\nu_2(a_1)$	$\nu_3(b_2)$	
Expt.	2806	1353	2865	Refs. [29,34]
Fitted empirical	2809	1353	2865	Ref. [14]
cc-pVQZ UCCSD(T) + VPT2	2819	1367	2871	Ref. [32]
aug-cc-pCVQZ ROCCSD(T) + VPT2	2806	1362	2860	Ref. [6]
aug-cc-pCVQZ ROCCSD(T) + NRLH	2805	1358	2860	Ref. [6]
aug-cc-pCVQZ ROCCSD(T) + VAR	2809	1361	2863	Present work

[a] All CCSD(T) harmonic and anharmonic results are based on quadratic and quartic force field representations of the appropriate PESs, respectively.

vibrational perturbation theory (VPT2) calculations. The reliability of the underlying optimized Born–Oppenheimer equilibrium structures and the related anharmonic (quartic) force fields have been discussed several times before [32, 39–42].

The internal coordinate quartic force fields of $^3CH_2$ and $^1CH_2$, computed at the all-electron aug-cc-pCVQZ CCSD(T) level at their respective optimized geometries, thus eliminating the nonzero force dilemma [42], are used both in VPT2 and variational calculations. The $[r_e(CH), \angle_e(HCH)]$ structural parameters at this level are [1.075981 Å, 133.8483°] and [1.106907 Å, 102.1369°] for $^3CH_2$ and $^1CH_2$, respectively. The best available computational and the empirical estimates of the Born–Oppenheimer equilibrium structures of $^3CH_2$ and $^1CH_2$ show an almost perfect agreement for both states. For $^3CH_2$, the best empirical estimates are $r_e(CH) = $ 1.0753(3) Å and $\angle_e(HCH) = 133.93(1)°$ [14], while for $^1CH_2$ they are $r_e(CH) = 1.1066(3)$ Å and $\angle_e(HCH) = $ 102.37° [43]. For the variational calculations the all-electron aug-cc-pCVQZ CCSD(T) force fields, reported in Ref. [6] in full detail, have been slightly modified [44] by transforming them from a simple (STRE, STRE, BEND) representation to a (SPF, SPF, BEND) representation, where SPF stands for the Simons–Parr–Finlan [45,46] coordinate.

The fitted empirical PESs of Jensen and Bunker are employed both for $^3CH_2$ and $^1CH_2$, corresponding to the 'fitted' constants of Tables 2 and 5 of Ref. [14], respectively.

The CCSD(T) technique, with its approximate inclusion of triple excitations, overcomes the difficulty of a single-reference-based description of $^1CH_2$, which hindered early ab initio calculations of this electronic state even close to equilibrium [8]. This can be seen from the excellent agreement not only between the computed [6] and experimental [43] structural parameters, given above, but also in a similar comparison of the vibrational fundamentals. The excellent agreement in the computed and measured vibrational fundamentals ensures that the effective adiabatic vibrational zero-point energy of $^1CH_2$ should indeed be very close to 3612 cm^{-1} (Table 2), our computed value, based on a fully variational treatment involving the all-electron aug-cc-pCVQZ CCSD(T) quartic force field, which is a value in fact only 1 cm^{-1} away from the MORBID result of Jensen and Bunker [14] and only 9 cm^{-1} away from the latest result of Gu et al. [16].

3. Computation of rovibrational levels of CH₂

3.1. Second-order vibrational perturbation theory (VPT2)

The lengthy standard formulas resulting from second-order vibrational perturbation theory (VPT2) for the

computation of vibrational anharmonicities, and consequently anharmonic ZPEs, have been published several times [47–51]. Therefore, there is no need to reintroduce them here. It is mentioned only briefly that performance of ab initio electronic structure calculations for determining anharmonic vibrational energy levels and transitions through quartic force fields and VPT2 formulas have extensively been tested [49,50] with the result that for semirigid molecules these computations are able to yield highly accurate results, especially for species containing no hydrogens [52].

It must be stressed that there are problems with describing the ZPE of $^3CH_2$ with VPT2. VPT2 is only valid as long as each internal coordinate described is contained in a deep well. The PES of $^3CH_2$ is rather shallow along the bending mode, with the barrier to linearity being less than 2000 cm^{-1} and a bending frequency of only 963.1 cm^{-1}. Thus, for this state simple VPT2 offers a somewhat unreliable approach. This observation could be at least partially responsible for the larger than usual, around 50 cm^{-1}, overestimation [6] of the experimentally observed ν_2 value by the VPT2 approach for $^3CH_2$ (see relevant data of Table 2). Nevertheless, VPT2 results are expected to be perfectly reliable for the stretching modes.

3.2. Variational computations

The most effective way to compute lower-lying rovibrational energy levels of triatomic molecules involves a discrete variable representation (DVR) [53–60] of the rovibrational Hamiltonian. This choice enables the potential energy matrix elements to be evaluated very efficiently. The numerical efficiency of the method as a whole is best if one can choose an orthogonal coordinate system so that there are no cross-derivative terms in the kinetic energy operator. If this is possible, one can often find a set of basis functions in which the kinetic energy matrix elements can be evaluated analytically and speedily, yielding results that can easily be incorporated into the DVR framework.

Assuming that an orthogonal system is chosen, the rotation–vibration Hamiltonian, which incorporates the radial part of the Jacobian, is

$$\hat{H}_{rv} = -\frac{1}{2\mu_1} \frac{\partial^2}{\partial R_1^2} - \frac{1}{2\mu_2} \frac{\partial^2}{\partial R_2^2}$$

$$- \left(\frac{1}{2\mu_1 R_1^2} + \frac{1}{2\mu_2 R_2^2} \right) \left(\frac{1}{\sin\theta} \frac{\partial}{\partial\theta} \sin\theta \frac{\partial}{\partial\theta} - \frac{\hat{j}_z^2}{\sin^2\theta} \right)$$

$$+ \frac{1}{2\mu_1 R_1^2} (\hat{J}^2 - 2\hat{J}_z \hat{j}_z - \hat{J}_+ \hat{j}_- - \hat{J}_- \hat{j}_+)$$

$$+ V(R_1, R_2, \theta),$$

$$(1)$$

where μ_1 and μ_2 are effective masses related to the actual masses in a way that depends on how precisely the orthogonal coordinate system is chosen, R_1 and R_2 are two radial internal coordinates whose form may be chosen at will within the limits imposed by the coordinate orthogonality constraint, θ is the angle between the two radial coordinates, while $\hat{J}$ and $\hat{j}$ refer to the appropriate [60] rotational angular momenta. The molecular plane is the x–z plane with the y-axis perpendicular to it. One of the radial coordinates is taken to lie along the z-axis. The coordinate choices made determine the precise form of $\hat{j}_z$ and the physical meaning of the reciprocal radial operator $(2\mu_1 R_1^2)^{-1}$ multiplying the angular momentum term.

It is not always computationally best to make an orthogonal coordinate choice and even when making such a choice, one particular scheme can prove to be better than another, as can a particular choice of the positioning of the molecule in the frame. Great care in making appropriate choices must be exercised in order to perform effective variational calculations.

The present nuclear motion calculations are performed in the orthogonal Jacobi internal coordinates, choosing CH as the diatom defining the z-axis so that R_1 is the diatomic bond length and $\mu_1 R_1^2$ is the diatomic moment of inertia. This body-fixed reference frame corresponds to the R_1 embedding [60]. The coordinates and the embedding chosen proved to be effective for CH_2 though may be far from being optimal for other systems [61,62].

It is always useful to have in mind a suitable set of basis functions to set up the matrix representation of $\hat{H}_{rv}$. The details of the function choice should reflect the coordinate and embedding choices made. A typical basis function is written as

$$\chi_{n_1}(R_1)\chi_{n_2}(R_2)\Phi_\ell^K(\theta)C_{MK}^{Jp}(\varphi, \chi, \psi), \tag{2}$$

where $\{\chi_{n_j}(R_j)\}_{n_j=0}^{N_j-1}$, $j=1, 2$, represents a one-dimensional DVR basis of the radial coordinates (with $\{q_{i_j}\}_{i_j=1}^{N_j}$ quadrature points), $\{\Phi_\ell^K(\theta)\}_{\ell=K,K=(0/1)}^{L-1+K,J}$, where (0/1) refers to (odd/even) parity solutions (vide infra), form the associated Legendre-DVR basis, used exclusively in this study, ϕ, χ and ψ are the usual Euler angles [63], and C_{MK}^{Jp} is the rotation function (parity-adapted symmetric-top eigenfunctions) formed by combining the normalized Wigner rotation functions, $\mathfrak{D}_{M\pm K}^J$, as

$$C_{MK}^{Jp} = [2(1 + \delta_{K0})]^{-1/2}[\mathfrak{D}_{MK}^J + (-1)^{J+K+p}\mathfrak{D}_{M-K}^J], \tag{3}$$

where p stands for parity [63], while M and K are the usual quantum numbers corresponding to space- and body-fixed projections of the rotational angular momentum on the appropriate z-axes. Although the most common choice for the radial functions is the Laguerre-DVR basis, involving Morse-like functions, in the present work a Hermite–DVR basis is used for $\{\chi_{n_j}(R_j)\}_{n_j=0}^{N_j-1}$. For the present application, the two basis sets exhibited similar convergence characteristics.

The matrix elements of the radial derivative parts of the kinetic energy operator,

$$(\mathbf{K}^{\alpha\times\alpha})_{n_j,n_j'} = \langle\chi_{n_j}(R_j)| -\frac{1}{2\mu_j}\frac{\partial^2}{\partial R_j^2}|\chi_{n_j'}(R_j)\rangle, \tag{4}$$

can be obtained analytically [64], where $\alpha = N_1$ or N_2.

Representation of the angular derivative parts can be similarly calculated and represented in DVR form as

$$\mathbf{L}_K^{L\times L} = (\mathbf{T}_K^\theta)^{\mathrm{T}}\tilde{\mathbf{L}}\mathbf{T}_K^\theta, \tag{5}$$

where $(\tilde{\mathbf{L}})_{\ell\ell'} = \ell(\ell + 1)\delta_{\ell\ell'}$, $\ell = K, K+1, \ldots, L-1+K$, is a diagonal matrix and the $\mathbf{T}_K^\theta$ transformation matrix between the finite basis representation (FBR) and the DVR is built from the eigenvectors of the coordinate matrix $\mathbf{Q}_K$ having matrix elements

$$(Q_K)_{\ell,\ell'} = \langle P_\ell^K(\cos\theta)|\cos\theta|P_{\ell'}^K(\cos\theta)\rangle$$

$$= -\sqrt{\frac{(\ell + K)(\ell - K)}{(2\ell + 1)(2\ell - 1)}}\delta_{\ell,\ell'+1}$$

$$-\sqrt{\frac{(\ell - K + 1)(\ell + K + 1)}{(2\ell + 1)(2\ell + 3)}}\delta_{\ell,\ell'-1}, \tag{6}$$

where $\{P_\ell^K\}_{\ell=K}^{L-1+K}$ are the associated Legendre polynomials. Representations of the multiplicative operators expressed in radial coordinates, $(2\mu_j R_j^2)^{-1}$, $j=1$ or 2, are diagonal in the DVR:

$$(\mathbf{R}_j)_{n_j,n_j'} = \frac{1}{2\mu_j r_{n_j}^2}\delta_{n_j,n_j'}. \tag{7}$$

In the case of a Hermite–DVR basis

$$r_{n_j} = \frac{q_{n_j}}{q_{N_j}}\frac{R_j^{\max} - R_j^{\min}}{2} + \frac{R_j^{\max} + R_j^{\min}}{2}, \tag{8}$$

where q_{n_j}s are the appropriate Gaussian quadrature points. Consequently, all grid points are defined in the interval $[R_j^{\min}, R_j^{\max}]$. This way one can ensure that all grid points are in a physically meaningful region. Up to this point operators only for the pure vibrational motion have been considered [44]. The last term of the kinetic energy operator describes the rotational motion of the system.

For setting up the matrix representation of the last term of the kinetic energy operator of the rovibrational Hamiltonian we take advantage of the rotational functions C_{MK}^{Jp} which are eigenfunctions of $\hat{j}^2$ and $\hat{j}_z^2$ with eigenvalues proportional to $J(J+1)$ and K^2, respectively. Therefore, one has to set up the K-dependent matrix representation of $(2\mu_1 R_1^2)^{-1}[J(J+1) - 2K^2]$ for the R_1 embedding as:

$$(\tilde{\mathbf{R}}_1^K)_{n_1,n_1'} = \frac{J(J+1) - 2K^2}{2\mu_1 r_{n_1}^2}\delta_{n_1,n_1'}. \tag{9}$$

To compute the matrix elements of the terms involving the raising and lowering operators, note that the effect of these two operators on the chosen angular functions is

$$\hat{J}_+ C_{MK}^{Jp} = [2(1 + \delta_{K0})]^{-1/2}[\Lambda_{JK}^+ \mathfrak{D}_{MK+1}^J$$

$$+ (-1)^{J+K+p}\Lambda_{JK}^+ \mathfrak{D}_{M-K+1}^J] \qquad (10a)$$

and

$$\hat{J}_- C_{MK}^{Jp} = [2(1 + \delta_{K0})]^{-1/2}[\Lambda_{JK}^- \mathfrak{D}_{MK-1}^J$$

$$+ (-1)^{J+K+p}\Lambda_{JK}^- \mathfrak{D}_{M-K-1}^J]. \qquad (10b)$$

The FBR matrix of $(-\hat{J}_+\hat{j}_- - \hat{J}_-\hat{j}_+)$ is then written as

$$(\mathbf{B}_K^{\pm \text{FBR}})_{\ell, \ell \mp 1} = -(1 + \delta_{K0} + \delta_{K'0})^{1/2}\Lambda_{JK}^\pm \Lambda_{\ell K}^\pm, \qquad (11)$$

where $\Lambda_{\eta K}^\pm = \sqrt{\eta(\eta + 1) - K(K \pm 1)}$, η is either J or ℓ as appropriate, and all the unspecified matrix elements are equal to zero. The corresponding DVR matrix can be obtained as

$$\mathbf{B}_K^\pm = (\mathbf{T}_{K\pm 1}^\theta)^{\text{T}}\mathbf{B}_K^{\pm \text{FBR}}\mathbf{T}_K^\theta, \qquad (12)$$

where the $\mathbf{T}_{K\pm 1}^\theta$ and $\mathbf{T}_K^\theta$ are transformation matrices defined earlier.

To set-up the matrix representation of those parts of the Hamiltonian that involve rotational operators, it is useful to group the basis functions into separate sets of even and odd parity. Let $K_{\max}$ be $J+1$ and J for odd and even parity solutions, respectively, where J is the total rotational quantum number. In other words, the total rovibrational Hamiltonian matrix for a given J is built up of blocks (Fig. 1) and one cycles through K to build the Hamiltonian matrix, where K also denotes the index of this cycle, and for odd-parity energy levels K runs from 0 to J, while for even-parity solutions K runs from 1 to J.

The total rotation–vibration Hamiltonian matrix can be written as a sum of direct products, each of four matrices, and adding to it the diagonal potential matrix

$$\mathbf{H}^{\text{DVR}} = \mathbf{I}^{K_{\max} \times K_{\max}} \otimes \mathbf{K}^{N_1 \times N_1} \otimes \mathbf{I}^{N_2 \times N_2} \otimes \mathbf{I}^{L \times L}$$

$$+ \mathbf{I}^{K_{\max} \times K_{\max}} \otimes \mathbf{I}^{N_1 \times N_1} \otimes \mathbf{K}^{N_2 \times N_2} \otimes \mathbf{I}^{L \times L}$$

$$+ \sum_{K=(0/1)}^J [\mathbf{E}_{K,K}^{K_{\max} \times K_{\max}} \otimes \mathbf{R}_1^{N_1 \times N_1} \otimes \mathbf{I}^{N_2 \times N_2}$$

$$\otimes \mathbf{L}_K^{L \times L} + \mathbf{E}_{K,K}^{K_{\max} \times K_{\max}} \otimes \mathbf{I}^{N_1 \times N_1} \otimes \mathbf{R}_2^{N_2 \times N_2}$$

$$\otimes \mathbf{L}_K^{L \times L} + \mathbf{E}_{K,K}^{K_{\max} \times K_{\max}} \otimes \tilde{\mathbf{R}}_1^K \otimes \mathbf{I}^{N_2 \times N_2} \otimes \mathbf{I}^{L \times L}$$

$$+ \mathbf{E}_{K,K+1}^{K_{\max} \times K_{\max}} \otimes \mathbf{R}_1^{N_1 \times N_1} \otimes \mathbf{I}^{N_2 \times N_2} \otimes \mathbf{B}_K^+$$

$$+ \mathbf{E}_{K,K-1}^{K_{\max} \times K_{\max}} \otimes \mathbf{R}_1^{N_1 \times N_1} \otimes \mathbf{I}^{N_2 \times N_2} \otimes \mathbf{B}_K^-] + \mathbf{V}, \qquad (13)$$

where $\mathbf{I}^{\eta \times \eta}$ is the identity matrix of size $\eta \times \eta$. The $\mathbf{E}_{K,K}^{K_{\max} \times K_{\max}}$, $\mathbf{E}_{K,K-1}^{K_{\max} \times K_{\max}}$, and $\mathbf{E}_{K,K+1}^{K_{\max} \times K_{\max}}$ matrices are of size $K_{\max} \times K_{\max}$, having only one nonzero element equal to one at the element indicated by the subscripts. In a DVR the diagonal matrix of the potential energy operator $\hat{V}(R_1, R_2, \cos\theta)$ is formed as

$$(\mathbf{V})_{Kn_1 n_2 \ell, K'n_1' n_2' \ell'} = V(r_{n_1}, r_{n_2}, q_\ell^K)\delta_{Kn_1 n_2 \ell, K'n_1' n_2' \ell'}, \qquad (14)$$

where the K-dependent q_ℓ^K are the eigenvalues of $\mathbf{Q}_K$ [Eq. (6)].

The final Hamiltonian matrix, $\mathbf{H}^{\text{DVR}}$, is a $N_1 N_2 L(J + 1) \times N_1 N_2 L(J + 1)$- or $N_1 N_2 LJ \times N_1 N_2 LJ$-dimensional sparse symmetric matrix of special structure. Fig. 1 shows the structure of the Hamiltonian matrix, whereby

$$\mathbf{H}^{(K,K)} = \mathbf{K}^{N_1 \times N_1} \otimes \mathbf{I}^{N_2 \times N_2} \otimes \mathbf{I}^{L \times L} + \mathbf{I}^{N_1 \times N_1} \otimes \mathbf{K}^{N_2 \times N_2}$$

$$\otimes \mathbf{I}^{L \times L} + \tilde{\mathbf{R}}_1^K \otimes \mathbf{I}^{N_2 \times N_2} \otimes \mathbf{I}^{L \times L} + \mathbf{R}_1^{N_1 \times N_1}$$

$$\otimes \mathbf{I}^{N_2 \times N_2} \otimes \mathbf{L}_K^{L \times L} + \mathbf{I}^{N_1 \times N_1} \otimes \mathbf{R}_2^{N_2 \times N_2} \otimes \mathbf{L}_K^{L \times L} \qquad (15)$$

and

$$\mathbf{H}^{(K,K+1)} = \mathbf{R}_1^{N_1 \times N_1} \otimes \mathbf{I}^{N_2 \times N_2} \otimes \mathbf{B}_K^+ \text{ and}$$

$$\mathbf{H}^{(K,K-1)} = \mathbf{R}_1^{N_1 \times N_1} \otimes \mathbf{I}^{N_2 \times N_2} \otimes \mathbf{B}_K^- \qquad (16)$$
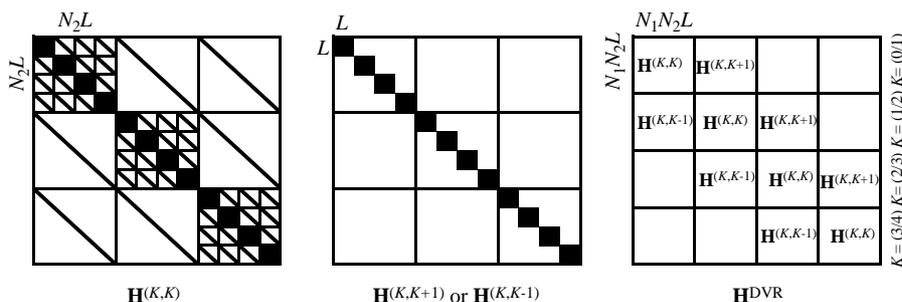

Fig. 1. Pictorial representation of the shape and the nonzero elements of the matrices appearing in Eqs. (13), (15), and (16) (for the sake of clarity, $N_1 = 3$ and $N_2 = 4$). In this figure, the total rovibrational Hamiltonian matrix, $\mathbf{H}^{\text{DVR}}$, is given for $J = (3/4)$ for (odd/even) parity.

One can take advantage of the sparsity and special structure of the Hamiltonian matrix by employing an iterative algorithm, in the present case that of Lanczos [65], specialized for sparse matrices for computation of the required eigenvalues.

The computer code developed as part of this study, based on Eqs. (1)–(16), is called DOPI3R as its predecessor vibrational counterpart was named DOPI3 [44].

4. Rotational transitions

The precision of theory that can be expected for variational computation of rotational transitions can be judged from results obtained for water [41,66]. There the rotational transitions could be reproduced on the order of 0.001 cm^{-1} using a high-quality purely ab initio PES [66]. Note, however, that this extensive PES of water, denoted as CVRQD [41], included relativistic [67,68], quantum electrodynamic (Lamb-shift) [69], DBOC [70], and non-adiabatic [71] effects, as well as a considerably better treatment than CCSD(T) of the valence and core correlation effects. Therefore, a similar precision cannot be expected in this study employing a much lower level of theory and quartic force field expansions of the Born–Oppenheimer PESs of $^3CH_2$ and $^1CH_2$.

4.1. $\tilde{X}^3B_1$ CH_2 and CD_2

To the best of our knowledge, all available rotational transitions measured for and in between vibrational states of $^3CH_2$ and $^3CD_2$ have been collected by Jensen and Bunker [14]. The empirical PES employed in this study was computed by the same authors [14] from all the known vibration–rotation data on $^3CH_2$. Their surface reproduces the observed transitions to better than 0.2 cm^{-1}. Therefore, there is no reason to include the variational results based on this PES in any of the tables of this paper. Our computed variational results are always compared to measured rotational transitions. Tables 3 and 4 show computed rotational transitions on the (000) states of $\tilde{X}^3B_1$ CH_2 and CD_2, respectively, and their residuals. Table 5 shows rotational transitions on the (010) state of $\tilde{X}^3B_1$ CH_2, while Table 6 shows similar data for the ν_2 band of $\tilde{X}^3B_1$ CD_2.

As is clear from Tables 3 and 4, the all-electron aug-cc-pCVQZ CCSD(T) quartic force field representation of the PES of $^3CH_2$ does not yield results of accuracy comparable to those obtained for water [41,66] for the observed rotational transitions. This is clearly due both to short-comings of the electronic structure approach applied for this highly flexible molecule and to the force field representation of the PES. Nevertheless, the results are reasonably accurate, none of the transitions on the (000) vibrational ground state of $^{12}CH_2$ and $^{12}CD_2$ deviate more than 1.1 and 0.6 cm^{-1}, respectively, from their experimental

Table 3
Representative calculated rotational transitions, in cm^{-1}, on the ground vibrational state (000) of $\tilde{X}^3B_1$ $^{12}CH_2$ and their deviations from experiment[a,b]

Transition	Calculated	Residual
$4_{04} \leftarrow 3_{13}$	2.876	0.566
$2_{12} \leftarrow 3_{03}$	14.229	−0.558
$5_{05} \leftarrow 4_{14}$	20.355	0.574
$1_{11} \leftarrow 2_{02}$	30.894	−0.553
$1_{10} \leftarrow 1_{01}$	63.334	−0.549
$2_{11} \leftarrow 2_{02}$	64.620	−0.545
$3_{12} \leftarrow 3_{03}$	66.577	−0.538
$4_{13} \leftarrow 4_{04}$	69.234	−0.530
$6_{15} \leftarrow 6_{06}$	76.810	−0.501
$1_{11} \leftarrow 0_{00}$	77.768	−0.553
$2_{12} \leftarrow 1_{01}$	92.267	−0.559
$4_{22} \leftarrow 5_{15}$	96.568	−0.975
$3_{22} \leftarrow 4_{13}$	96.697	−1.038
$5_{23} \leftarrow 5_{14}$	157.534	−1.045
$5_{42} \leftarrow 4_{31}$	381.342	−1.095
$6_{43} \leftarrow 5_{32}$	397.472	−1.096
$6_{42} \leftarrow 5_{33}$	397.478	−1.096
$7_{44} \leftarrow 6_{33}$	413.604	−1.097
$7_{43} \leftarrow 6_{34}$	413.621	−1.097

[a] The standard notation [63] $J_{K_aK_c}$ has been invoked in denoting the pure rotational levels involved in the transitions. The variational nuclear motion calculations utilized the all-electron aug-cc-pCVQZ CCSD(T) quartic force field in (SPF, SPF, BEND) coordinates as a PES. The residuals are defined as calculated − experimental.
[b] The experimental data are taken from Ref. [14].

Table 4
Representative calculated rotational transitions, in cm^{-1}, on the ground vibrational state (000) of $\tilde{X}^3B_1$ $^{12}CD_2$ and their deviations from experiment[a,b]

Transition	Calculated	Residual
$1_{11} \leftarrow 2_{02}$	16.962	−0.230
$1_{10} \leftarrow 1_{01}$	33.317	−0.239
$2_{11} \leftarrow 2_{02}$	33.866	−0.238
$3_{12} \leftarrow 3_{03}$	34.701	−0.235
$1_{11} \leftarrow 0_{00}$	40.710	−0.245
$2_{12} \leftarrow 1_{01}$	48.121	−0.252
$3_{13} \leftarrow 2_{02}$	55.277	−0.260
$4_{22} \leftarrow 5_{15}$	58.417	−0.527
$3_{22} \leftarrow 4_{13}$	59.580	−0.553
$2_{21} \leftarrow 3_{12}$	68.463	−0.554
$5_{15} \leftarrow 4_{04}$	68.865	−0.278
$5_{23} \leftarrow 5_{14}$	90.393	−0.576
$4_{22} \leftarrow 4_{13}$	91.449	−0.572
$3_{21} \leftarrow 3_{12}$	92.336	−0.569
$2_{20} \leftarrow 2_{11}$	93.027	−0.566
$3_{22} \leftarrow 3_{13}$	95.452	−0.560
$4_{23} \leftarrow 4_{14}$	96.593	−0.558
$3_{22} \leftarrow 2_{11}$	116.863	−0.583

[a] The standard notation [63] $J_{K_aK_c}$ has been invoked in denoting the pure rotational levels involved in the transitions. The variational nuclear motion calculations utilized the all-electron aug-cc-pCVQZ CCSD(T) quartic force field in (SPF, SPF, BEND) coordinates as a PES. The residuals are defined as calculated − experimental.
[b] The experimental data are taken from Ref. [14].

Table 5

Representative calculated rotational transitions, in cm^{-1}, on the (010) band of $\tilde{X}^3B_1$ $^{12}CH_2$ and their deviations from experiment[a,b]

Transition	Calculated	Residual
$4_{14} \leftarrow 5_{23}$	804.565	−0.385
$4_{13} \leftarrow 5_{24}$	817.823	−0.321
$5_{24} \leftarrow 6_{33}$	817.654	−1.513
$3_{13} \leftarrow 4_{22}$	823.574	−0.383
$3_{12} \leftarrow 4_{23}$	831.447	−0.350
$4_{04} \leftarrow 5_{15}$	832.830	0.724
$4_{22} \leftarrow 5_{33}$	833.869	−1.512
$4_{23} \leftarrow 5_{32}$	833.843	−1.524
$2_{11} \leftarrow 3_{22}$	845.616	−0.368
$3_{22} \leftarrow 4_{31}$	849.962	−1.537
$3_{21} \leftarrow 4_{32}$	849.971	−1.535
$1_{11} \leftarrow 2_{20}$	859.030	−0.388
$2_{02} \leftarrow 3_{13}$	860.170	0.678
$1_{10} \leftarrow 2_{21}$	860.321	−0.382
$2_{20} \leftarrow 3_{31}$	866.012	−1.178
$1_{01} \leftarrow 2_{12}$	874.443	0.661
$4_{14} \leftarrow 4_{23}$	883.614	−0.403
$3_{13} \leftarrow 3_{22}$	886.669	−0.384
$2_{12} \leftarrow 2_{21}$	888.972	−0.388
$2_{11} \leftarrow 2_{20}$	892.772	−0.373
$3_{12} \leftarrow 3_{21}$	894.207	−0.353
$4_{04} \leftarrow 4_{13}$	896.053	0.657
$5_{14} \leftarrow 5_{23}$	898.214	−0.299
$2_{02} \leftarrow 2_{11}$	901.748	0.654
$5_{24} \leftarrow 5_{33}$	912.307	−1.519
$5_{23} \leftarrow 5_{32}$	912.344	−1.508
$4_{23} \leftarrow 4_{32}$	912.781	−1.534
$4_{22} \leftarrow 4_{31}$	912.800	−1.528
$3_{22} \leftarrow 3_{31}$	913.153	−1.543
$3_{13} \leftarrow 2_{20}$	933.825	−0.387
$2_{02} \leftarrow 1_{11}$	935.474	0.662
$3_{03} \leftarrow 2_{12}$	951.667	0.690
$4_{14} \leftarrow 5_{05}$	1034.728	−1.951
$2_{12} \leftarrow 3_{03}$	1070.006	−1.955
$1_{11} \leftarrow 2_{02}$	1086.878	−1.955
$2_{11} \leftarrow 2_{02}$	1120.620	−1.936
$3_{12} \leftarrow 3_{03}$	1122.498	−1.920
$5_{14} \leftarrow 5_{05}$	1128.377	−1.863
$1_{11} \leftarrow 0_{00}$	1133.875	−1.832
$2_{12} \leftarrow 1_{01}$	1148.042	−1.957
$3_{13} \leftarrow 2_{02}$	1161.673	−1.955
$4_{14} \leftarrow 3_{03}$	1174.665	−1.956

[a] The standard notation [63] $J_{K_aK_c}$ has been invoked in denoting the pure rotational levels involved in the transitions. The variational nuclear motion calculations utilized the all-electron aug-cc-pCVQZ CCSD(T) quartic force field in (SPF, SPF, BEND) coordinates as a PES. The residuals are defined as calculated − experimental.
[b] The experimental data are taken from Ref. [14].

counterparts (Tables 3 and 4). It is interesting to observe that the residual errors of the transitions do not change appreciably with J, they scatter either around −0.5, +0.5, or −1.0 cm^{-1} for the parent isotopolog $^{12}CH_2$ (Table 3). This behavior of the residuals is not easily explicable though it is clearly connected to tendencies in the K_a dependence of the error in the computed rotational term values.

Table 6

Representative calculated rotational transitions, in cm^{-1}, on the ground vibrational state (010) of $\tilde{X}^3B_1$ $^{12}CD_2$ and their deviations from experiment[a,b]

Transition	$^{12}CD_2$	
	Calculated	Residual
$1_{11} \leftarrow 2_{02}$	45.517	−0.347
$2_{11} \leftarrow 2_{02}$	61.836	−0.887
$3_{12} \leftarrow 3_{03}$	62.744	−0.898
$1_{11} \leftarrow 0_{00}$	68.534	−0.903
$2_{12} \leftarrow 1_{01}$	75.925	−0.901
$3_{13} \leftarrow 2_{02}$	83.073	−0.907
$4_{14} \leftarrow 3_{03}$	89.974	−0.930
$2_{21} \leftarrow 3_{12}$	115.699	−1.372
$3_{21} \leftarrow 3_{12}$	139.512	−1.385
$2_{20} \leftarrow 2_{11}$	140.066	−0.731
$2_{21} \leftarrow 2_{12}$	141.785	−1.371
$2_{21} \leftarrow 1_{10}$	156.485	−1.382
$2_{20} \leftarrow 1_{11}$	157.024	−0.844

[a] The standard notation [63] $J_{K_aK_c}$ has been invoked in denoting the pure rotational levels involved in the transitions. The variational nuclear motion calculations utilized the all-electron aug-cc-pCVQZ CCSD(T) quartic force field in (SPF, SPF, BEND) coordinates as a PES. The residuals are defined as calculated − experimental.
[b] The experimental data are taken from Ref. [14].

4.2. $\tilde{a}^1A_1$ CH_2

Tables 7 and 8 show the computed rotational transitions on the (000) and (010) states of $\tilde{a}^1A_1$ CH_2 and their residuals [34], respectively. There is nothing unusual about the rotational term values and transitions of this state, they show the precision that can be expected from a high-quality quartic force field representation of the PES. In particular, for a given J the deviation between computed and measured term values increases considerably with K_a, a discrepancy which gets reflected in the computed transition energies.

Table 7

Representative calculated rotational transitions, in cm^{-1}, on the ground vibrational state (000) of $\tilde{a}^1A_1$ $^{12}CH_2$ and their deviations from experiment[a]

Transition	$^{12}CH_2$	
	Calculated	Residual
$2_{02} \leftarrow 0_{00}$	53.757	0.142
$6_{25} \leftarrow 4_{41}$	60.262	−2.048
$3_{13} \leftarrow 1_{11}$	80.407	0.086
$3_{31} \leftarrow 1_{11}$	182.739	1.351
$4_{22} \leftarrow 2_{02}$	186.325	1.215
$5_{32} \leftarrow 4_{14}$	212.842	1.600
$4_{32} \leftarrow 2_{12}$	225.333	1.419
$4_{40} \leftarrow 2_{20}$	259.014	2.673
$5_{42} \leftarrow 3_{22}$	299.309	3.019
$5_{50} \leftarrow 3_{30}$	336.856	3.067
$7_{25} \leftarrow 5_{05}$	351.797	2.607
$6_{52} \leftarrow 4_{32}$	374.946	3.216

[a] The standard notation [63] $J_{K_aK_c}$ has been invoked in denoting the pure rotational levels involved in the transitions. The variational nuclear motion calculations utilized the all-electron aug-cc-pCVQZ CCSD(T) quartic force field in (SPF, SPF, BEND) coordinates as a PES. The residuals are defined as calculated − experimental. See Ref. [34] for the experimental data.

Table 8
Representative calculated rotational transitions, in cm^{-1}, on the ground vibrational state (010) of $\tilde{a}^1A_1$ $^{12}CH_2$ and their deviations from experiment[a]

Transition	Calculated	Residual
$2_{11} \leftarrow 1_{11}$	45.501	−0.762
$3_{12} \leftarrow 1_{10}$	101.768	0.488
$5_{14} \leftarrow 4_{14}$	138.510	0.865
$3_{30} \leftarrow 2_{12}$	165.025	2.785
$6_{15} \leftarrow 5_{15}$	171.663	0.743
$4_{31} \leftarrow 3_{13}$	193.493	2.923
$5_{32} \leftarrow 4_{14}$	227.868	3.068
$7_{16} \leftarrow 5_{14}$	233.463	0.891
$6_{52} \leftarrow 5_{32}$	302.285	4.515
$6_{51} \leftarrow 5_{33}$	306.714	4.444

[a] The standard notation [63] $J_{K_aK_c}$ has been invoked in denoting the pure rotational levels involved in the transitions. The variational nuclear motion calculations utilized the all-electron aug-cc-pCVQZ CCSD(T) quartic force field in (SPF, SPF, BEND) coordinates as a PES. The residuals are defined as calculated−experimental. See Ref. [34] for the experimental data.

The residuals for the rotational transitions of $\tilde{a}^1A_1$ CH_2 are highly similar to those obtained for the ground electronic state, i.e. the internal coordinate quartic force field representations of the PESs of $\tilde{X}^3B_1$ and $\tilde{a}^1A_1$ CH_2 are reasonably accurate and able to reproduce the measured rovibrational transitions with an expected precision. Therefore, (a) the precision of the equilibrium structure and the vibrational fundamentals for $^1CH_2$ and $^3CH_2$ should be highly similar; and (b) none of the rotational data calls into question the utility of these PES representations for predicting the stretching fundamentals and the ZPEs of either state.

5. Stretching fundamentals and zero-point energy of $^3CH_2$

The vibrational fundamentals of $\tilde{a}^1A_1$ CH_2, 2805.9 (a_1), 1352.6 (a_1), and 2864.5 (b_2) cm^{-1}, have been measured [29,34] directly and accurately. As is clear from the VPT2 results of Ref. [6] and from Tables 1 and 2 of this study, for semirigid $^1CH_2$ the all-electron aug-cc-pCVQZ CCSD(T) force field, when used within the standard VPT2 formulas, yields highly accurate vibrational fundamentals and, consequently, a zero-point energy of similar accuracy. This statement is further supported by the NRLH results of Ref. [6] and by the fully variational vibrational results of this study (Tables 1 and 2). The final ZPE estimate of $^1CH_2$, 3605 ± 15 cm^{-1}, corresponds to the first eigenvalue of the converged variational nuclear motion calculation of this study based on the all-electron aug-cc-pCVQZ CCSD(T) quartic force field, corrected by the sum of half the differences between the computed and measured fundamentals. It is expected that the error estimate given is a conservative 2σ estimate, augmented to include a correction due to the Renner–Teller effect [16].

There is no reason not to expect a similar accuracy for the all-electron aug-cc-pCVQZ CCSD(T) quartic force field in representing the lower part of the PES of $^3CH_2$. Nevertheless, as this electronic state does not satisfy the requirement for semirigidity, the straight application of VPT2 formulas leads to a wrong bending fundamental. However, for the stretching fundamentals nonrigidity should present no problems. The nuclear motion calculations in 1D (NRLH) and 3D (DOPI3R) support this view. Namely, while the VPT2 and the fully variational and NRLH bending fundamentals differ by 44 cm^{-1}, similar differences for the stretching fundamentals do not exceed 5 cm^{-1}. As expected, the NRLH and VPT2 stretching fundamentals differ by less than 4 cm^{-1}. These observations add to the confidence in the calculated fundamentals of the present study.

All published fully ab initio high-level computations of the harmonic frequencies of $^3CH_2$ indicate (for a partial list see Table 1) that once a reasonably large Gaussian basis set, of at least triple-zeta quality, and an extensive treatment of electron correlation, of at least CCSD(T) quality, is used for the electronic structure calculations, the equilibrium structure and the harmonic frequencies of $^3CH_2$ change very little. The differences among CCSD(T) results also depend very little on whether an unrestricted or a restricted formalism has been used for the open-shell computations. This also suggests that the CCSD(T) level of theory provides a dependable estimate of the harmonic vibrational fundamentals of $^3CH_2$.

As noted several times before, see, e.g. Ref. [42], the anharmonic contribution to the vibrational fundamentals can be computed rather dependably at relatively low levels of theory. Therefore, the anharmonic correction results to the stretching fundamentals obtained in this study at the aug-cc-pCVQZ CCSD(T) level are expected to be highly reliable. Furthermore, it is generally accepted that anharmonic stretching fundamentals computed with the help of VPT2 formulas have a precision usually exceeding that of variational treatments using the same quartic force field. In the present case, the largest difference between the VPT2 and variational fundamentals is less than 5 cm^{-1} (Table 2). Consequently, the computed anharmonic stretching fundamentals should be accurate.

In summary, the stretching vibrational fundamentals of the $\tilde{X}^3B_1$ electronic state of CH_2, 3035 ± 7 (a_1) and 3249 ± 7 (b_2) cm^{-1}, have been established with confidence. The ZPE of this state, 3733 ± 10 cm^{-1}, is also well established through the present variational nuclear motion calculations. This ^{3}ZPE estimate corresponds to the first eigenvalue of the converged variational nuclear motion calculation of this study based on the all-electron aug-cc-pCVQZ CCSD(T) quartic force field, corrected by half of the difference between the computed and measured bending fundamental. It is expected that the error estimate given is a conservative 2σ estimate.

6. On the determination of $T_0(\tilde{a}^1A_1)$

Since one of the strongest arguments in favor of the correctness of ^{3}ZPE calculated in this study ab initio involves $T_0(\tilde{a}^1A_1)$, it is worth checking how $T_0(\tilde{a}^1A_1)$ was obtained. Most importantly, $T_0(\tilde{a}^1A_1)$ has not been measured directly and its determination [11,14,16], yielding $3147 \pm 5 \text{ cm}^{-1}$, employed a mixture of experimental and theoretical components.

The direct spectroscopic measurements leading to $T_0(\tilde{a}^1A_1)$ are laser-magnetic-resonance (LMR) transitions involving known rovibrational levels of $^1CH_2$. Normally, singlet levels cannot be observed in LMR experiments because their energies are unchanged by a magnetic field. The existence of the observed transitions can only be explained by assuming that the singlet levels are perturbed by rovibrational levels of $^3CH_2$ through spin–orbit interactions.

Let the perturbed singlet and the perturbing triplet levels have energies, relative to the rovibrational ground state of $^3CH_2$, $E_1 + T_0$ and E_3, respectively. From the spectroscopic observations, combined with pure ab initio determinations of the singlet-triplet spin-orbit matrix elements, it was possible to obtain $T_0 = E_3 - E_1 - \Delta E = 3147 \text{ cm}^{-1}$, using unperturbed values of E_3 and E_1 calculated with MORBID [30] and the fitted empirical PESs of Bunker and Jensen [14], and a ΔE obtained by manipulation of a 2×2 matrix to include coupling between the two levels.

The empirical PESs employed in the determination of $T_0(\tilde{a}^1A_1)$ are the same as those utilized in this study. The accuracy of the stretching part of the $^3CH_2$ PES has been questioned in this study. Fortunately, the states with energies E_3 involve bending vibrational excitation only so it is likely that the MORBID calculations gave accurate energies for them. Furthermore, although the stretching levels of $^3CH_2$ do change following the present treatments, the ab initio vibronic matrix elements (Table 10 of Ref. [11]) indicate that the stretching fundamentals have much smaller spin-orbit coupling matrix elements with the $\tilde{a}^1A_1$ (0 0 0) state than do the highly rotationally excited (0 2 0) and (0 3 0) bending states utilized in obtaining $T_0(\tilde{a}^1A_1)$. Therefore, the empirical determination of $T_0(\tilde{a}^1A_1)$ is to be trusted though further studies might show small deviations from the present mean value.

7. Conclusions

The 0–0 transition between the lowest two electronic states of CH_2 has been established empirically as $T_0(\tilde{a}^1A_1) = 3147 \pm 5 \text{ cm}^{-1}$ [11,14,16]. A value of $T_e(\tilde{a}^1A_1) = 3262^{+29}_{-16}$ cm^{-1} was obtained in a highly accurate computation [6], by two of the authors of the present study, after establishing the all-electron complete basis set (CBS) full configuration interaction (FCI) limit and augmenting this result with relativistic and diagonal Born−Oppenheimer corrections (DBOC) in the spirit of the focal-point approach (FPA).

The high-accuracy empirical T_0 and the ab initio T_e values are only compatible if not the available empirical estimates [10–16], ranging from -171 to $+100 \pm 140 \text{ cm}^{-1}$, are used for the difference between the singlet and triplet ZPEs but computational, purely ab initio estimates, obtained either variationally or perturbationally. The required nuclear motion calculations, performed in Ref. [6] and here, include both the nonrigid-rotation-large-amplitude-internal-motion Hamiltonian (NRLH) approach of Szalay and a fully variational treatment. They both employed accurate quartic force field representations of the potential energy surfaces (PES) of $\tilde{X}^3B_1$ and $\tilde{a}^1A_1$ CH_2. The fully perturbational calculations remained within the framework of VPT2. All ab initio estimates of the vibrational fundamentals and ZPEs of $^3CH_2$ and $^1CH_2$ are very similar. Furthermore, the vibrational fundamentals for semirigid $^1CH_2$ are in excellent agreement with the available experimental data, none of the deviations are larger than 8 cm^{-1}. The computed bending fundamentals of nonrigid $^3CH_2$ are also in good accord with the only experimentally available fundamental of $^3CH_2$, except, as expected, when the VPT2 approach is used for its determination. These observations suggest that the stretching fundamentals of $^3CH_2$ should also be accurate, corresponding to a highly accurate estimate of the ZPE of this electronic state.

To further check the accuracy of the quartic force field representations of the PESs, rotational transitions have been computed using a newly developed code, DOPI3R, described here in detail. While the fitted empirical PES of $^3CH_2$ obtained by Jensen and Bunker [14] reproduces, in a converged variational calculation, the available experimental rotational transitions very accurately these transitions proved to be insufficient to fix the true form of the PES of $^3CH_2$. Consequently, the stretching fundamentals obtained from this empirically refined PES are in quite large error, deviating up to 44 cm^{-1} from the dependable pure ab initio results. The similar precision of the prediction of the rotational term values observed for $^3CH_2$ and $^1CH_2$ provide further evidence about the claimed high precision of the force field PES of $^3CH_2$.

While the present calculations provide accurate estimates of the stretching fundamentals, 3035 ± 7 (a_1) and 3249 ± 7 (b_2) cm^{-1}, of $^3CH_2$ facilitating their eventual experimental detection considerably, the low intensity of these bands [72] should hinder their detection in the near future.

The detailed high-level ab initio investigation of the vibrational fundamentals and the rotational transitions of the lowest triplet and singlet states of methylene allows us to obtain the following dependable ZPE estimates: ^{3}ZPE$ = 3733 \pm 10 \text{ cm}^{-1}$, ^{1}ZPE$ = 3605 \pm 15 \text{ cm}^{-1}$, and ΔZPE$ = 128 \pm 18 \text{ cm}^{-1}$.

Acknowledgements

References

[1] H.F. Schaefer III, Science 231 (1986) 1100.

[2] G. Herzberg, Proc. R. Soc. Lond. A 262 (1961) 291.

[3] L. Halberstadt, J.R. McNesby, J. Am. Chem. Soc. 89 (1967) 3417.

[4] W. Carr, T.W. Eder, M.G. Topor, J. Chem. Phys. 53 (1970) 4716.

[5] P.F. Zittel, G.B. Ellison, S.V. O'Neil, E. Herbst, W.C. Lineberger, W.P. Reinhardt, J. Am. Chem. Soc. 98 (1976) 3731.

[6] A.G. Császár, M.L. Leininger, V. Szalay, J. Chem. Phys. 118 (2003) 10631.

[7] C.D. Sherrill, M.L. Leininger, T.J. Van Huis, H.F. Schaefer III, J. Chem. Phys. 108 (1998) 1040.

[8] A. Kalemos, T.H. Dunning Jr., A. Mavridis, J.F. Harrison, Can. J. Chem. 82 (2004) 684.

[9] B. Ruscic, J.E. Boggs, A. Burcat, A.G. Császár, J. Demaison, R. Janoschek, J.M.L. Martin, M. Morton, M.J. Rossi, J.F. Stanton, P.G. Szalay, P.R. Westmoreland, T. Bérces, J. Phys. Chem. Ref. Data 34 (2005) 573.

[10] T.J. Sears, P.R. Bunker, A.R.W. McKellar, J. Chem. Phys. 77 (1982) 5363.

[11] A.R.W. McKellar, P.R. Bunker, T.J. Sears, K.M. Evenson, R.J. Saykally, S.R. Langhoff, J. Chem. Phys. 79 (1983) 5251.

[12] D.G. Leopold, K.K. Murray, A.E.S. Miller, W.C. Lineberger, J. Chem. Phys. 83 (1985) 4849.

[13] A.D. McLean, P.R. Bunker, R.M. Escribano, P. Jensen, J. Chem. Phys. 87 (1987) 2166.

[14] P. Jensen, P.R. Bunker, J. Chem. Phys. 89 (1988) 1327.

[15] D.C. Comeau, I. Shavitt, P. Jensen, P.R. Bunker, J. Chem. Phys. 90 (1989) 6491.

[16] J.-P. Gu, G. Hirsch, R.J. Buenker, M. Brumm, G. Osmann, P.R. Bunker, P. Jensen, J. Mol. Struct. 517,518 (2000) 247.

[17] V.J. Barclay, I.P. Hamilton, P. Jensen, J. Chem. Phys. 99 (1993) 9709.

[18] A.G. Császár, G. Tarczay, M.L. Leininger, O.L. Polyansky, J. Tennyson, W.D. Allen, in: J. Demaison, K. Sarka (Eds.), Spectroscopy from Space, NATO ASI Series C: Mathematical and Physical Sciences (2001), pp. 317–339.

[19] A.G. Császár, W.D. Allen, Y. Yamaguchi, H.F. Schaefer III, in: P. Jensen, P.R. Bunker (Eds.), Computational Molecular Spectroscopy, Wiley, Chichester, 2000, pp. 15–68.

[20] W.D. Allen, A.L.L. East, A.G. Császár, in: J. Laane, M. Dakkouri, B. Van der Veken, H. Oberhammer (Eds.), Structures and Conformations of Nonrigid Molecules, NATO ASI Series C: Mathematical and Physical Sciences, Kluwer, Dordrecht, 1993.

[21] A.G. Császár, W.D. Allen, H.F. Schaefer III, J. Chem. Phys. 108 (1998) 9751.

[22] V. Szalay, J. Mol. Spectrosc. 128 (1988) 24.

[23] V. Szalay, J. Chem. Phys. 92 (1990) 3633.

[24] G. Tarczay, A.G. Császár, W. Klopper, V. Szalay, W.D. Allen, H.F. Schaefer III, J. Chem. Phys. 110 (1999) 11971.

[25] The NRLH method amounts to an adiabatic separation of the bending and stretching motions. The bending motion is described by a geometrically defined curvilinear coordinate, while rectilinear displacement coordinates describe the stretching motions. The effect of stretching vibrations on the bending motion is taken into account by second-order perturbation theory.

[26] A.R. Hoy, P.R. Bunker, J. Mol. Spectry. 52 (1974) 439; R. Beardsworth, P.R. Bunker, P. Jensen, W.P. Kraemer, J. Mol. Spectry. 118 (1986) 50.

[27] G. Herzberg, J.W.C. Johns, Proc. R. Soc. Lond. A 295 (1966) 107.

[28] D. Feldman, K. Meier, R. Schmiedl, K.H. Welge, Chem. Phys. Lett. 60 (1978) 30.

[29] H. Petek, G.J. Nesbitt, P.R. Ogilby, C.B. Moore, J. Phys. Chem. 87 (1983) 5367.

[30] P. Jensen, J. Mol. Spectry. 128 (1988) 478; P. Jensen, J. Chem. Soc. Faraday Trans. 84 (1988) 1315.

[31] J.-S.K. Yu, S.-y. Chen, C.-H. Yu, J. Chem. Phys. 118 (2003) 582.

[32] A. Tajti, P.G. Szalay, A.G. Császár, M. Kállay, J. Gauss, E.F. Valeev, B.A. Flowers, J. Vazquéz, J.F. Stanton, J. Chem. Phys. 121 (2004) 11599.

[33] M.D. Marshall, A.R.W. McKellar, J. Chem. Phys. 85 (1986) 3716.

[34] H. Petek, D.J. Nesbitt, C.B. Moore, F.W. Briss, D.A. Ramsay, J. Chem. Phys. 86 (1987) 1189.

[35] T.H. Dunning Jr., J. Chem. Phys. 90 (1989) 1007.

[36] R.A. Kendall, T.H. Dunning Jr., R.J. Harrison, J. Chem. Phys. 96 (1992) 6796.

[37] The (aug-)cc-p(C)VXZ basis sets were obtained from the Extensible Computational Chemistry Environment Basis Set Database, Version 1.0, as developed by the Molecular Science Computing Facility, Environmental and Molecular Sciences laboratory, which is part of the Pacific Northwest Laboratory, P.O. Box 999, Richland, Washington 99352, USA and funded by the U.S. Department of Energy. The Pacific Northwest laboratory is a multiprogram laboratory operated by Battelle Memorial Institute for the U.S. Department of Energy under Contract No. DE-AC06-76RLO 1830.

[38] K. Raghavachari, G.W. Trucks, J.A. Pople, M. Head-Gordon, Chem. Phys. Lett. 157 (1989) 479.

[39] K.L. Bak, J. Gauss, P. Jørgensen, J. Olsen, T. Helgaker, J.F. Stanton, J. Chem. Phys. 114 (2001) 6548.

[40] A.G. Császár, in: P.v.R. Schleyer, N.L. Allinger, T. Clark, J. Gasteiger, P.A. Kollmann, H.F. Schaefer III, P.R. Schreiner (Eds.), The Encyclopedia for Computational Chemistry vol. 1, Wiley, Chichester, 1998, pp. 13–30.

[41] A.G. Császár, G. Czakó, T. Furtenbacher, J. Tennyson, V. Szalay, S.V. Shirin, N.F. Zobov, O.L. Polyansky, J. Chem. Phys. 122 (2005) 214305.

[42] W.D. Allen, A.G. Császár, J. Chem. Phys. 98 (1993) 2983.

[43] H. Petek, G.J. Nesbitt, D.C. Darwin, P.R. Ogilby, C.B. Moore, D.A. Ramsay, J. Phys. Chem. 91 (1989) 6566.

[44] G. Czakó, T. Furtenbacher, A.G. Császár, V. Szalay, Mol. Phys. 102 (2004) 2411.

[45] G. Simons, R.G. Parr, J.M. Finlan, J. Chem. Phys. 59 (1973) 3229.

[46] A. Kratzer, Z. Phys. 3 (1920) 289; E. Fues, Ann. Phys. (Berlin) 80 (1926) 367.

[47] H.H. Nielsen, Phys. Rev. 60 (1941) 794; H.H. Nielsen, Phys. Rev. 68 (1945) 181; H.H. Nielsen, Rev. Mod. Phys. 23 (1951) 90.

[48] I.M. Mills, in: K.N. Rao, C.W. Mathews (Eds.), Molecular Spectroscopy: Modern Research, Academic Press, New York, 1972, pp. 115–140.

[49] D.A. Clabo Jr., W.D. Allen, R.B. Remington, Y. Yamaguchi, H.F. Schaefer III, Chem. Phys. 123 (1988) 187.

[50] W.D. Allen, Y. Yamaguchi, A.G. Császár, D.A. Clabo Jr., R.B. Remington, H.F. Schaefer III, Chem. Phys. 145 (1990) 427.

[51] M. Schuurman, S. Muir, W.D. Allen, H.F. Schaefer III, J. Chem. Phys. 120 (2004) 11586.

[52] S. Bailleux, M. Bogey, C. Demuynck, J.L. Destombes, N. Dujardin, Y. Liu, A.G. Császár, J. Chem. Phys. 107 (1997) 8317.

[53] C. Leforestier, J. Chem. Phys. 94 (1991) 6388.

[54] X.T. Wu, E.F. Hayes, J. Chem. Phys. 107 (1997) 2705.

[55] J. Tennyson, J.R. Henderson, N.G. Fulton, Comp. Phys. Comm. 86 (1995) 175.

[56] G. Czakó, V. Szalay, A.G. Császár, T. Furtenbacher, J. Chem. Phys. 122 (2005) 024101.

[57] G. Czakó, V. Szalay, A.G. Császár, J. Chem. Phys. submitted for publication (2005).

[58] M.J. Bramley, T. Carrington Jr., J. Chem. Phys. 99 (1993) 8519.

[59] J.C. Light, I.P. Hamilton, J.V. Lill, J. Chem. Phys. 82 (1985) 1400; J.C. Light, T. Carrington Jr., Adv. Chem. Phys. 114 (2000) 263.

[60] B.T. Sutcliffe, J. Tennyson, Int. J. Quant. Chem. 39 (1991) 183.

[61] J. Tennyson, M.A. Kostin, H.Y. Mussa, O.L. Polyansky, R. Prosmiti, Phil. Trans. Royal Soc. Lond. A 358 (2000) 2419.

[62] J. Tennyson, M.A. Kostin, P. Barletta, G.J. Harris, J. Ramanlal, O.L. Polyansky, N.F. Zobov, Comp. Phys. Comm. 163 (2004) 85.

[63] R.N. Zare, Angular Momentum, Wiley, New York, 1988.

[64] V. Szalay, J. Chem. Phys. 99 (1993) 1978.

[65] C. Lanczos, J. Res. Narl. Bur. Stand. 45(1950)255. J.K. Cullum, R.A. Willoughby, Lanczos Algorithms for Large Symmetric Eigenvalue Computations, Birkhauser, Boston, 1985.

[66] O.L. Polyansky, A.G. Császár, S.V. Shirin, N.F. Zobov, P. Barletta, J. Tennyson, D.W. Schwenke, P.J. Knowles, Science 299 (2003) 539.

[67] A.G. Császár, J.S. Kain, O.L. Polyansky, N.F. Zobov, J. Tennyson, Chem. Phys. Lett. 293 (1998) 317 (312, (1999) 613 (E)).

[68] G. Tarczay, A.G. Császár, W. Klopper, H.M. Quiney, Mol. Phys. 99 (2001) 1769.

[69] P. Pyykkö, K.G. Dyall, A.G. Császár, G. Tarczay, O.L. Polyansky, J. Tennyson, Phys. Rev. A 63 (2001) 024502.

[70] N.F. Zobov, O.L. Polyansky, C.R. Le Sueur, J. Tennyson, Chem. Phys. Lett. 260 (1996) 381.

[71] D.W. Schwenke, J. Phys. Chem. A 105 (2001) 2352.

[72] P. Jensen, J. Mol. Spectry. 132 (1988) 429.